JACS
JOURNAL OF THE AMERICAN CHEMICAL SOCIETY
pubs.acs.org/JACS
Article

Real-Time Observation of Conformational Changes and Translocation of Endogenous Cytochrome c within Intact Mitochondria

Jianhua Zhan, Danyun Zeng, Xiong Xiao, Zhongpei Fang, Tao Huang, Beibei Zhao, Qinjun Zhu, Caixiang Liu, Bin Jiang, Xin Zhou, Conggang Li, Lichun He, Daiwen Yang, Maili Liu,* and Xu Zhang*

Cite This: J. Am. Chem. Soc. 2024, 146, 4455−4466

Read Online

ACCESS | Metrics & More | Article Recommendations | Supporting Information

ABSTRACT: Cytochrome c (cyt c) is a multifunctional protein with varying conformations. However, the conformation of cyt c in its native environment, mitochondria, is still unclear. Here, we applied NMR spectroscopy to investigate the conformation and location of endogenous cyt c within intact mitochondria at natural isotopic abundance, mainly using widespread methyl groups as probes. By monitoring time-dependent chemical shift perturbations, we observed that most cyt c is located in the inner mitochondrial membrane and partially unfolded, which is distinct from its native conformation in solution. When suffering oxidative stress, cyt c underwent oxidative modifications due to increasing reactive oxygen species (ROS), weakening electrostatic interactions with the membrane, and gradually translocating into the inner membrane spaces of mitochondria. Meanwhile, the lethality of oxidatively modified cyt c to cells was reduced compared with normal cyt c. Our findings significantly improve the understanding of the molecular mechanisms underlying the regulation of ROS by cyt c in mitochondria. Moreover, it highlights the potential of NMR to monitor high-concentration molecules at a natural isotopic abundance within intact cells or organelles.

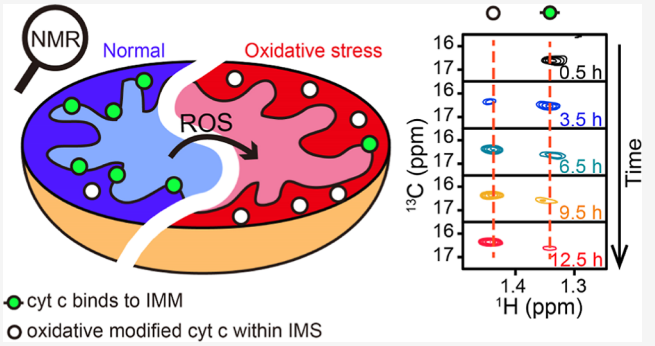

INTRODUCTION

Cytochrome c (cyt c) is a highly conserved heme protein that transfers electrons in the respiration chain of mitochondria.[1,2] It also acts as a scavenger to resist oxidation damage,[3] making it a useful first-aid medicine for hypoxia.[4] In addition, cyt c induces cell apoptosis when released to the cytosol under certain stimuli, such as DNA damage or oxidative stress.[5,6]

To meet multifunctional needs, the conformation of cyt c shows flexibility and high adaptability.[7] Extensive studies have been conducted to elucidate its various conformations under different solution circumstances.[1] The structure of cyt c comprises five α-helices, two short antiparallel β-sheets, and a conserved heme group that is deeply embedded in the hydrophobic center.[8] Typically, the iron of heme is six-coordinate in its native state. H18 and M80 axially bond to the iron that expels solvent from the center.[9] When the surrounding environment changes, the Fe-M80 bond can be easily disrupted, leading to a partially unfolded conformation of cyt c with high peroxidase activity.[10] For instance, the Fe-M80 contact is substituted by Fe−K79 or Fe−K73 at high pH.[11] Furthermore, the conformation of cyt c is also influenced by temperature and pressure.[12,13]

In mitochondria, where cyt c is mainly located in eukaryotic cells, more specific factors influence the structure and function of cyt c. At first, mitochondria keep redox environments inside for the respiration of cells, which generate reactive oxygen species (ROS).[14,15] These ROS, such as H_2O_2, oxidize cyt c at M80, Y67, and lysines from surface to depth, leading to the rupture of the Fe-M80 bond and promotion of the peroxidase activity.[16,17] Second, it has been well-studied that the electrostatic interactions between cyt c and cardiolipin (CL) in the mitochondria membrane can cause an expansion of the structure of cyt c and rupture of the Fe-M80 bond as well.[18,19] Brazhe *et al.* detected that cyt c contains a ferric heme in intact mitochondria by surface-enhanced Raman spectroscopy,[20] while the tertiary structure of the protein and potential alterations in mitochondria remain unknown.

Probing the structures of proteins in cells and organelles is very challenging. The development of in-cell fluorescent probes,[21,22] electron paramagnetic resonance (EPR),[23−25]

Received: September 17, 2023
Revised: January 24, 2024
Accepted: January 24, 2024
Published: February 9, 2024

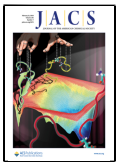

https://doi.org/10.1021/jacs.3c10216
J. Am. Chem. Soc. 2024, 146, 4455−4466

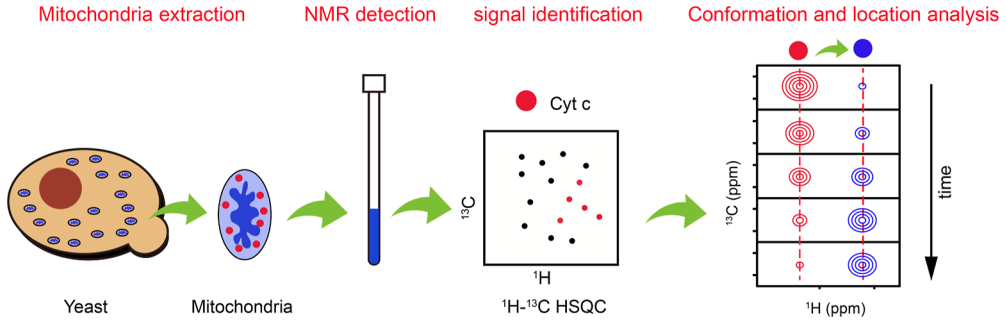

Figure 1. Scheme of the strategy for detecting the conformation and translocation of endogenous cyt c within mitochondria.

nuclear magnetic resonance (NMR),[26−28] and other technologies have provided great insights into the conformations of proteins *in vivo*. The investigation of various advanced sample preparation techniques,[29−31] such as protein overexpression, isotopic labeling, and electroporation technique, has empowered NMR as a formidable tool for *in situ* protein detection.[26−28] This technique has even been used to probe the conformation of proteins in mitochondria.[32] However, certain proteins that are challenging to express render these biomolecular techniques less effective, thereby constraining the utility of NMR. Moreover, there are doubts regarding the artificial enrichment of proteins within cells due to the potential for inducing unknown effects, such as the occurrence of the "protein burden" effect.[33−36]

In this work, naturally occurring conformations of cyt c were investigated in yeast mitochondria by using NMR spectroscopy (Figure 1). With a concentration range of 0.5−5 mM in mitochondria,[37,38] cyt c has the potential to be detected by NMR directly under natural isotopic abundance. ^{1}H−^{13}C NMR spectra demonstrate that the conformation of cyt c in mitochondria is significantly different from that of its native state in solution. The protein is partially unfolded, with a five-coordinated heme, and mainly binds to CL in the inner mitochondrial membrane (IMM). Real-time tracking of the protein using NMR reveals that cyt c undergoes oxidative modification under oxidative stress, followed by release from IMM, and its protein concentration increases in the intermembrane space (IMS) of mitochondria. Furthermore, the oxidatively modified cyt c exhibits less depression in cell growth, suggesting that the oxidative modification of cyt c protects the cell against apoptosis.

MATERIALS AND METHODS

Materials. CL, digitonin, Janus green B, and D_2O were purchased from Sigma-Aldrich (Merck, Burlington, MA, USA). The DCFH-DA kit, BCA Protein Assay Kit, MTT cell proliferation and cytotoxicity detection kit, and MitoTracker Red CMXRos were obtained from Beyotime Biotechnology (Shanghai, China). H_2O_2 and glycerol were purchased from Sinopharm Chemical Reagent Co, Ltd. (Shanghai, China). The mitochondria and cyt c were prepared in fresh 0.1 M sodium phosphate buffer (PBS) with pH 7.4.

Extraction of Mitochondria. Mitochondria were extracted from wild-type yeast cell strain BY4741, following a protocol described before.[39] Yeast was cultured in YEPD media (1% yeast extract, 2% peptone, and 2% glucose) for 48 h, and differential centrifugation and sucrose density gradient centrifugation were performed to extract crude mitochondria and high-purity mitochondria from the cells. The concentration of the isolated mitochondria was measured using the BCA Protein Assay Kit. All the experiments on mitochondria samples were conducted within 2−3 h after the extraction.

Separation of the Intermembrane Space and Inner Mitochondrial Membrane. IMS and IMM were separated by following a previously reported protocol.[40] The protein in the IMS was released by dissolving the outer mitochondrial membrane (OMM) using digitonin, and the supernatant was collected after 10000 g of centrifugation for 30 min. Digitonin is a nonionic detergent commonly used to separate mitoplast (IMM and matrix) from OMM.[40,41] Electrostatic interaction drives the interaction between cyt c and CL, and therefore the remaining precipitates were treated with 150 mM NaCl to release the rest of the cyt c from IMM.[42] The released cyt c was then obtained by collecting the supernatant after another round of 10000 g of centrifugation for 30 min.

Preparation of Cyt c. The yeast iso-1 cyt c used in this study was labeled with ^{15}N and ^{13}C and expressed in *Escherichia coli* BL21(DE_3). Purification was carried out using a two-step method involving a cation exchange column and size-exclusion chromatography column.[43] Ferrous and ferric cyt c were prepared for NMR detection by adding extra sodium L-ascorbate (SLA) and $K_3[Fe(CN)_6]$ into 0.1 M PBS buffer (pH 7.4), respectively.

Preparation of the CL Liposome. The CL liposome was prepared according to a reported protocol.[44] A 5 mL ethanol of CL was evaporated under a vacuum at 318 K to form an adherent film, which was then dissolved in 1 mL of precooled 0.1 M PBS solution at 277 K. The dissolved solution was sonicated in an ice bath for 15 min to obtain uniform CL liposomes on ice. The particle size and uniformity of the prepared liposomes were checked by dynamic light scattering (DynaPro NanoStar, Wyatt, Santa Barbara, CA, USA).

Detection of the Activity and Integrity of Extracted Mitochondria. The commonly used mitochondrial staining kit, Janus green B (0.2%), was utilized to visualize intact mitochondria. The integrity of the mitochondrial membrane was assessed using a MitoTracker Red CMXRos dye (20 nM). A stock of mitochondria with a total protein concentration of 1 mg/mL was prepared, then divided into five EP tubes, and incubated at 30 °C. For every 3 h, one aliquot was taken out, separated into two pools, and then stained by Janus green B and MitoTracker Red CMXRos dye, respectively. After being stained, the samples were further diluted to get a suitable concentration for observation. All staining results were viewed with a Nikon Eclipse Ts2R microscope (Nikon Corporation, Japan). The profiles of light intensities were plotted and analyzed by the software (NIS-Elements D 5.10.00) associated with the Nikon microscope.

Detection of the Functionality of Extracted Mitochondria. Succinate dehydrogenase in functional mitochondria can metabolize and reduce 3-(4,5-dimethylthiazol-2-yl)-2,5-diphenyltetrazolium bromide (MTT).[45] The process is accompanied by the production of blue-purple formazana, which is insoluble in water. The formazana particles can be dissolved and colored with isopropyl alcohol. So, the color of formazana particles can indicate the functionality of mitochondria mixing with MTT.

A stock of mitochondria with a total protein concentration of 5 mg/mL was prepared and aliquoted into 15 tubes. All samples were kept at 30 °C until three tubes were taken out every 3 h. The three tubes of samples were used as parallel tests. MTT was added into each tube following the kit instructions, and isopropyl alcohol was added

https://doi.org/10.1021/jacs.3c10216
J. Am. Chem. Soc. 2024, 146, 4455−4466

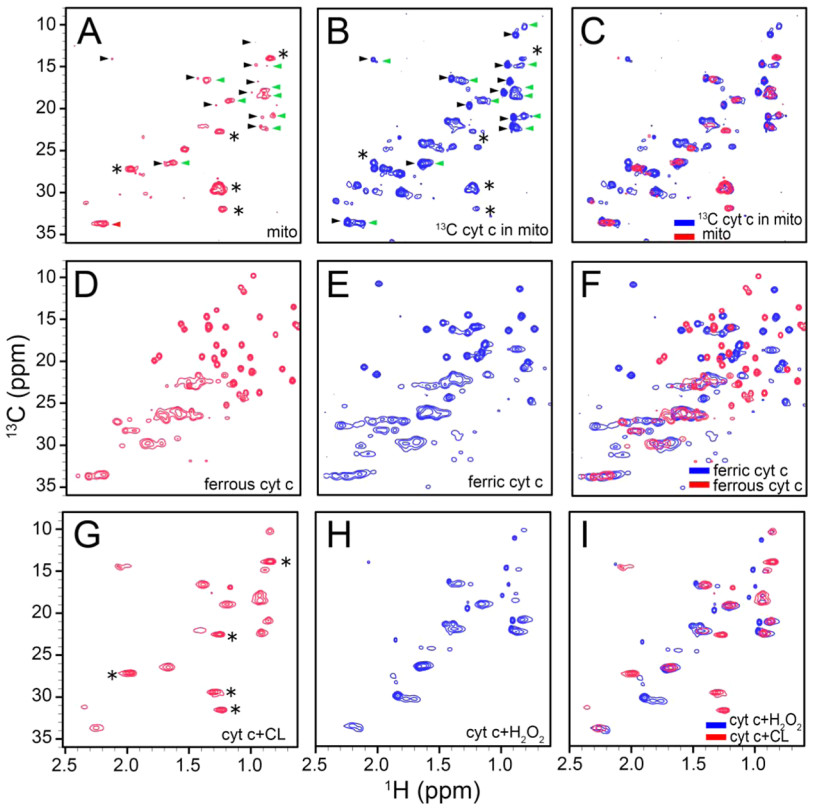

Figure 2. ^{1}H−^{13}C HSQC spectra of intact mitochondria and cyt c under various conditions. (A,B) Spectra of intact mitochondria without and with ^{13}C-labeled cyt c, respectively. (C) Overlay of (A,B). (D,E) Spectra of ferrous and ferric cyt c at a concentration of 0.1 mM, respectively. (F) Overlay of (D,E). (G,H) Spectra of 0.1 mM cyt c in the presence of 3.2 mM CL liposome and 0.5 mM H_2O_2, respectively. (I) Overlay of (G,H). (The green arrows represent one set of cyt c signals in mitochondria, which is the same as those bound to CL, the black arrows represent another set of cyt c signals in mitochondria, which is the same as those mixed with H_2O_2, and the asterisks represent other signals primarily originating from lipids in mitochondria).

after a 4 h incubation. Finally, UV absorbance around 570 nm was measured when the particles were completely dissolved in samples using a SpectraMax i3x multimode plate reader (Molecular Devices, San Jose, CA, USA).

Measurement of the Oxygen Consumption Rate of Extracted Mitochondria. Oxygen consumption rate (OCR) is one of the main indexes of respiration. It can be used to evaluate the metabolic status of mitochondria.[46,47] OCR of mitochondria was measured at Shanghai Fuda Testing Technology Group Co., Ltd. (Shanghai, China) by using a Seahorse Energy Metabolism Analyzer (Agilent Technologies, XFe24, USA). The mitochondria stock with a total protein concentration of 2 mg/mL was kept at 30 °C. For every 3 h, the OCR was recorded with three parallel samples.

Identification of the Cyt c in Living Mitochondria. To confirm the NMR signals from cyt c in mitochondria, ^{15}N and ^{13}C-labeled cyt c were introduced into mitochondria *via* electroporation, as described previously.[48,49] The mitochondria with protein concentrations of 20 mg/mL were divided into 100 μL aliquots, mixed with cyt c, and then electroporated using an Eppendorf Electroporator (Hamburg, Germany) at 1250 V in a cold electroporation cuvette with a 2 mm gap (Bio-Rad). It is important to notice that any remaining cyt c after electroporation was removed through multiple centrifugations.

Detection of the Carbonylation of Cyt c. Contents of carbonyl on cyt c were detected using 2, 4-DNPH kits and manipulated following the kit instructions. The proteins were reacted with 2, 4-DNPH, and the UV absorbance around 370 nm was measured using a SpectraMax i3x multimode plate reader (Molecular Devices, San Jose, CA, USA), according to the kit instructions.

Detection of the Internal ROS in Mitochondria. To identify ROS within the mitochondria, we utilized DCFH-DA kits and followed the procedures outlined below: the fluorescent dye was mixed with the mitochondrial solution, which had a protein concentration of 20 mg/mL, at a volume ratio of 1:1000. After 20 min of incubation at 303 K, the fluorescence of this mixture was then measured using a SpectraMax i3x multimode plate reader.

NMR Experiments. The mitochondria were suspended in 0.1 M PBS (pH 7.4) with 10% D_2O, at a final protein concentration of 20 mg/mL for NMR determination. All NMR experiments were conducted at 303 K on a Bruker Avance III 700 MHz NMR spectrometer equipped with a TXI cryoprobe. 2D ^{1}H−^{13}C HSQC spectra were acquired with spectral widths of 20.00 and 40.00 ppm for ^{1}H and ^{13}C, respectively, using 2048 and 128 complex points. The number of scans was 32. For high-resolution HSQC spectra used to identify the homonuclear scalar coupling between adjacent carbons, the spectral width of the ^{13}C dimension was 15.00 ppm. All NMR experimental data were processed with Bruker Topspin 4.0.1 software (Bruker, Billerica, MA, USA).

EPR Experiments. A 0.5 mM cyt c sample and a stock of mitochondria with a total protein concentration of 30 mg/mL were prepared in 20 mM HEPES buffer with 10% glycerol (pH 7.0), respectively. The samples were transferred into 4 mm quartz tubes and flash-frozen using liquid nitrogen for about 5 min before being put into an EPR spectrometer. EPR spectra were recorded at 10 K on an X-band EPR spectrometer (CIQTEK-EPR100) under the following conditions: a microwave frequency of 9.736 GHz, a microwave power of 0.2 mW, a modulation frequency of 100 kHz, a modulation amplitude of 1 G, and a time constant of 100 ms. The data processing and baseline calibration were completed by Origin 9.1.

Observation of the Effect of Cyt c on the Growth of Yeast Cells. The yeast was cultured to an OD of 2.0 in 10 mL of liquid

https://doi.org/10.1021/jacs.3c10216
J. Am. Chem. Soc. 2024, 146, 4455−4466

YEPD medium and then equally divided into several groups for various experimental conditions. The yeast cells were electroporated with 0.5 mM cyt c treated with varying concentrations of H_2O_2 in the SEM buffer (250 mM sucrose, 1 mM EDTA, 10 mM MOPS-KOH, pH 7.2), while the control group received the same amount of buffer solution. The yeast was then grown in a solid and liquid YEPD culture medium. The number of yeast cells was recorded throughout different durations of culturing. The solid medium was photographed, and cells of the liquid medium were counted using a blood cell count plate.

RESULTS AND DISCUSSION

Endogenous Cyt c within Intact Mitochondria Can Be Detected by NMR. The methyl group on the protein surface serves as an excellent probe for characterizing protein conformation at a natural isotope abundance. This was convincingly demonstrated by Jagger *et al.*, who utilized NMR to directly observe the conformation of a 52 kDa protein at natural isotopic abundance isolated from human plasma, thereby highlighting the powerful utility of methyl detection NMR in probing proteins within complex environments while preserving their native isotopic composition.[50]

In the cellular environment, methyl groups in the side chain may be less affected and, therefore, still detectable in the spectrum. To illustrate this, the enlarged $^1H-^{13}C$ HSQC NMR spectra shown in Figure 2 highlight the signals of proteins in high-field regions, and the full spectra are shown in Figure S1. In this spectral region, the signals directly acquired on intact yeast mitochondria predominantly originate from methyl groups (Figure 2A). This can be attributed to three equivalent protons present in the methyl group, which rotate rapidly around a connecting C−C bond, rendering them more detectable by NMR compared to other functional groups. Hence, the employment of $^1H-^{13}C$ NMR has emerged as a reliable approach for investigating proteins at their native isotopic abundances within complex environments.

To confirm the methyl signals are from cyt c inside mitochondria, we introduced ^{13}C-labeled cyt c into mitochondria by electroporation, and the corresponding area of the $^1H-^{13}C$ HSQC spectra is exhibited in Figure 2B. Compared with Figure 2A, the peaks in the two spectra are nearly identical, while most peaks simultaneously display increases in intensities in the spectrum of mitochondria in the presence of ^{13}C-labeled cyt c (indicated by triangle). The signals overlap in Figure 2C. In addition, when collecting $^1H-^{13}C$ HSQC experiments without carbon decoupling during acquisition periods, the majority of signals gradually showed a pair of split peaks in the flank according to rising concentrations of electroporated ^{13}C-labeled cyt c (Figure S2). Since the peak splitting was caused by homonuclear $^2J_{C,C}$ coupling between adjacent ^{13}C atoms, which was observable in ^{13}C-labeled proteins only,[51] the results indicate that the chemical shifts of original cyt c in mitochondria are consistent with of artificially introduced ^{13}C-cyt c, and the increments of peak intensities in the spectrum in Figure 2B are contributed by the labeled cyt c. In addition, the signal intensities of cyt c in the mitochondria extracted from yeast with cyt c gene knockout were obviously reduced compared to those in the mitochondria from wild-type yeast cells (Figure S3). Therefore, it is proven that the NMR resonances shown in Figure 2A belong to methyl groups of cyt c naturally in intact mitochondria.

Some signals showed no increase in intensities after the introduction of ^{13}C-labeled cyt c (indicated by an asterisk), indicating other preserved contents of mitochondria than cyt c. For example, the signal identification of CL, a substantial mitochondrial component, was further verified by comparing the $^1H-^{13}C$ HSQC spectrum of mitochondria with the spectrum of pure CL (Figure S4). Besides, the absence of signals in the $^1H-^{15}N$ HSQC spectrum of ^{15}N-labeled cyt c brought into mitochondria indicates that cyt c did not get degraded (Figure S5).

To better understand the conformation of cyt c in intact mitochondria, $^1H-^{13}C$ HSQC spectra of cyt c in various environments were acquired. In comparison with the spectra of native ferrous and ferric cyt c in dilute solution (Figure 2D,E), the chemical shifts of cyt c in mitochondria are different from those in either of these two states, showing significantly lower chemical shift dispersion, indicating that the conformation of cyt c in mitochondria is different from that in solution. The results suggest that the conformation of cyt c is influenced by the internal environment of mitochondria.

In mitochondria, the conformational transitions of cyt c can occur through two distinct pathways: interaction with CL at the IMM[52] and oxidation induced by elevated levels of ROS.[16] Observation of $^1H-^{13}C$ HSQC spectra of cyt c in solutions containing CL liposomes or H_2O_2 reveals limited chemical shift dispersion in Figure 2E,F, which is coincident with the presence of partially unfolded structures, as evidenced by CD and UV−visible spectra. These findings were also affirmed by our previous study, in which we established that cyt c assumes a partially unfolded state with ferric heme within the CL membrane or H_2O_2 environment, underscoring the influence of both environmental factors on cyt c conformation within mitochondria.[53]

It deserves to be noted that the spectrum of cyt c in mitochondria (Figure 2A) also shows poor chemical shift dispersion, and some of its signals overlap with those in the presence of CL liposome (indicated by red triangle), while some others overlap with those in the presence of H_2O_2 (indicated by black triangle). The former signals exhibit much higher intensities than the latter ones. These results all indicate that, in mitochondria, cyt c mainly adopts partially unfolded conformations, and they primarily bind to the IMM with some undergoing oxidative modification by ROS.

The supernatant of the mitochondria was checked using NMR after the aforementioned NMR detection within 2 h. No signal was detected, indicating that all of the signals mentioned above originated from cyt c within mitochondria (Figure S6). In our previous study, we assigned the side chain signals of ferric and ferrous cyt c using the 3D NMR technique.[54] By tracking chemical shift changes in these references, we assigned most of the resonances detected in mitochondria. Resonances were mainly methyl groups located in flexible loops on the negatively charged or uncharged surfaces of cyt c away from the CL binding site (Figure S7). This finding suggests that methyl groups are suitable for describing conformational changes in proteins in intact cells due to their flexibility and sensitivity.[55]

In addition, EPR experiments were performed to verify the iron state of cyt c within the mitochondria. EPR is a well-established tool for investigating the conformation of cyt c in various conditions.[56−58] The EPR spectra of both ferric cyt c and mitochondria samples are depicted in Figure S8. The detection of a high-spin EPR signal corresponding to ferric iron in the mitochondria signifies the presence of cyt c in the ferric state within the mitochondria. This supported our NMR spectral findings that ferric forms of cyt c were observed,

https://doi.org/10.1021/jacs.3c10216
J. Am. Chem. Soc. 2024, 146, 4455−4466

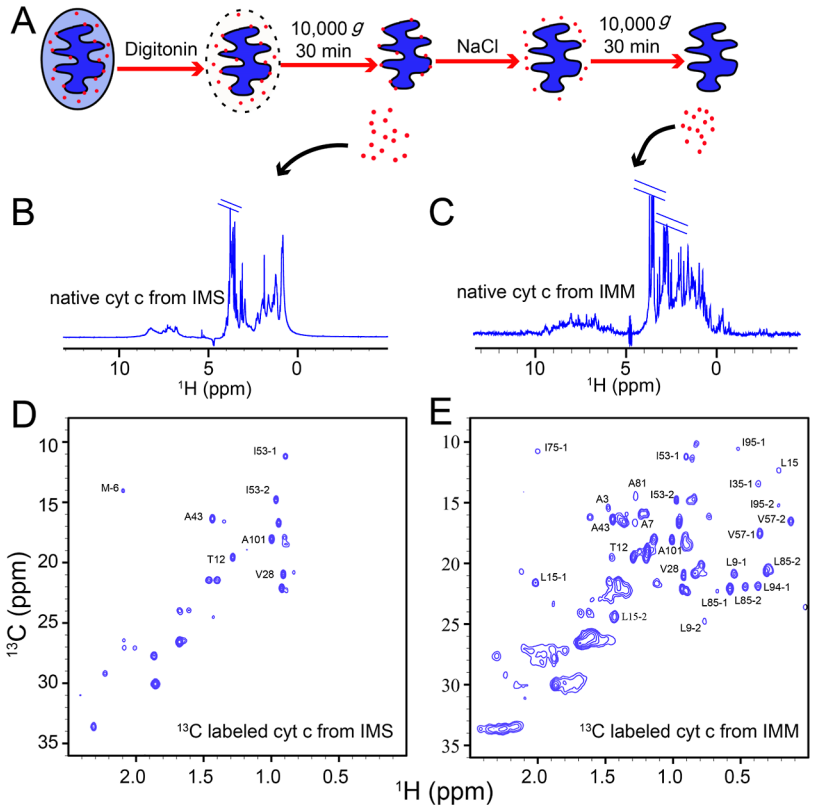

Figure 3. Cyt c in various locations of mitochondria. (A) Diagram of the separation process of cyt c from mitochondria. (B,C) 1D ^{1}H spectra of isolated cyt c from IMS and IMM, respectively. (The two diagonal lines cover some strong signals that may come from small molecules of metabolites). (D,E) 2D ^{1}H−^{13}C HSQC spectra of ^{13}C-labeled cyt c re-extracted from IMS and IMM, respectively.

suggesting that cyt c mainly exists in the ferric state within mitochondria. This outcome is plausible, given that ferric cyt c levels are known to increase subsequent to interactions with lipids such as CL on IMM or due to exposure to agents like H_2O_2.[59,60]

Cyt c Adopts Different Conformations Depending on the Locations within Mitochondria. The conformation of cyt c may vary, depending on its location. To determine its location within mitochondria, the IMS and IMM were separated and detected by using NMR. Figure 3A depicts the separation process. OMM had dissolved during the operation, which was confirmed by testing mitochondrial membrane potential using MitoTracker Red CMXRos (Figure S9).

To prove the success of the separation of cyt c from mitochondria, SDS-PAGE was first applied. The result showed a band in accordance with the molecular weight of cyt c in both lanes of samples gained from IMS and IMM, respectively (data not shown). Then NMR experiments were performed on the two samples separately. It was found that the ^{1}H NMR spectra of IMS and IMM are different from each other. Some of the resonances in the high-field region are identical to those of purified cyt c, and especially the signals from heme are distinguishable, implying that cyt c was successfully derived. Moreover, the signals of cyt c from the IMM are well dispersed, while peaks of cyt c from IMS are dispersed poorly (Figure 3B,C). These results indicate that cyt c extracted from the IMS still maintains a partially unfolded conformation, whereas cyt c gained from the IMM can restore the folded structure. Due to the low NMR sensitivity to proteins at natural isotope abundance, and some other components that simultaneously isolated with cyt c may bother the spectra, we did not further acquire 2D NMR spectra on these two samples.

To increase the sensitivity of the NMR detection of cyt c, 0.5 mM ^{13}C-labeled cyt c was electroporated into mitochondria. The ^{1}H−^{13}C HSQC spectra of cyt c extracted again from IMS and IMM are presented in Figure 3D,E, respectively. Both spectra show clear resonances of cyt c, demonstrating the existence of cyt c not only in the IMM but also in the IMS.

The NMR spectrum of cyt c in the IMS is distinct from that in a dilute solution (Figure 3D), despite the same pH and ionic concentration. The spectrum shows poor chemical shift dispersion and overlaps with one set of cyt c resonances in the presence of H_2O_2, implying a partially unfolded structure. Oxidative modification of residues on proteins is known to occur when exposed to H_2O_2,[17,61] so cyt c in IMS may undergo oxidative modification due to the high content of ROS in mitochondria.[14] Oxidative modification on lysine residues reduces the positive charge on the surface of cyt c,[62] disrupting its electrostatic interactions with CL,[63] and then leading to the release of cyt c into IMS. Whereas, the spectrum of cyt c released from the IMM with the addition of 150 mM NaCl shows a chemical shift dispersion pattern as a folded cyt c, with most resonances overlapping with ferric cyt c (Figure 2E). These findings indicate that cyt c in the IMM is ferric and can be refolded upon release into solution.[42]

To confirm that unfolded cyt c in IMS is ROS induced, ^{1}H−^{13}C HSQC spectra were used to examine the conformation transition of cyt c induced by the CL liposome and H_2O_2 in the presence of 150 mM NaCl (Figure S10). Results showed that while H_2O_2-induced unfolded cyt c remained unfolded in the presence of NaCl, CL-induced unfolded cyt c

https://doi.org/10.1021/jacs.3c10216
J. Am. Chem. Soc. 2024, 146, 4455−4466

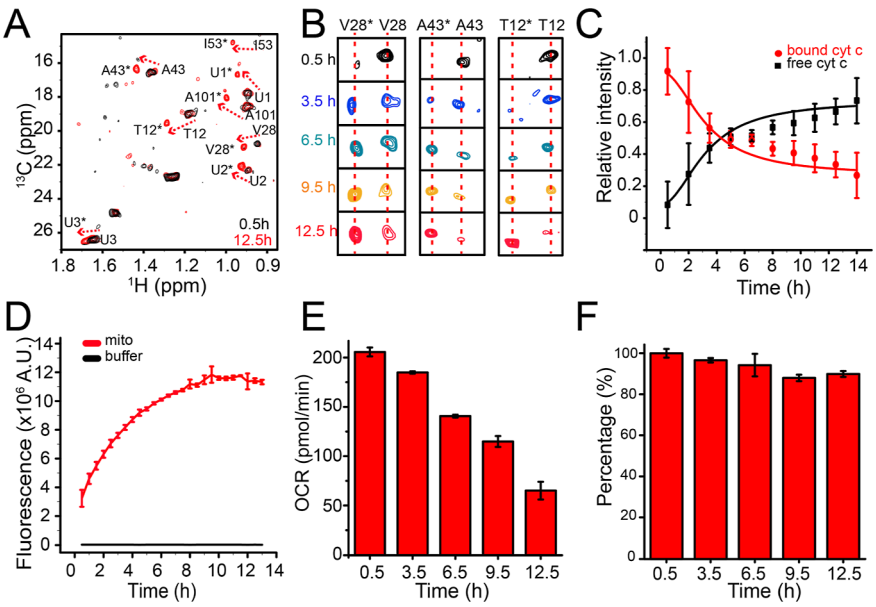

Figure 4. Changes of cyt c in intact mitochondria over time. (A) $^{1}H-^{13}C$ HSQC spectra of yeast mitochondria were taken at 0.5 and 12.5 h after the extraction, with labeled resonance assignments. Resonance marked with and without asterisks represents free cyt c in IMS and bound cyt c in IMM, respectively. "U" means unassigned resonances. (B) Changes in selected cyt c resonances in real-time. (C) Relative peak intensities of free and bound cyt c over time. (D) Fluorescence changes of ROS in living mitochondria over time. (E) OCR of mitochondria at different time points. (F) Monitoring of the functionality of mitochondria at different time points. Each column represents the percentage of 570 nm UV absorbance of each time point compared to the 0.5 h time point. Mitochondria at 0.5 h are considered 100% active. The mitochondria were incubated in five sealed EP tubes at 30 °C to simulate and monitor the sample condition during the real-time NMR experiments.

was refolded with the addition of NaCl, suggesting that released cyt c in IMS may undergo oxidative modification leading to an unrecoverable structure.

In addition, the redox state of cyt c in the IMM was further investigated by ^{1}H NMR and UV−vis spectroscopy. As a result of the paramagnetic effect of ferric iron, the NMR peaks of heme methyl groups (around 30−35 ppm) and M80 methyl group (−23.5 ppm) of cyt c exhibit specific chemical shift distributions in the ferric state. As illustrated in Figure S11, the ^{1}H NMR spectra of native cyt c isolated from the IMM displayed these characteristic chemical shifts. Meanwhile, in Figure S12, we observed the distinctive absorbance peaks of ferric cyt c at 410 and 527 nm in the UV−vis spectrum, which is the sign of ferric cyt c.[17] These results align with the detection of ferric iron in mitochondria *via* EPR analysis, further indicating the predominance of the ferric state of iron in cyt c within mitochondria.

Real-Time Observation of the Conformation and Translocation of Natural Cyt c in Mitochondria. It is known that cyt c function is relevant to its locations, and translocation of cyt c has been identified as a crucial step in apoptosis.[64] Monitoring the relative levels of cyt c binding to the IMM and free in the IMS (bound and free states) should help to understand the role of cyt c in apoptosis. Real-time NMR spectra of intact mitochondria were obtained to meet the purpose. Intact mitochondria were extracted from yeast and monitored for over 12 h. Figure 4A shows the $^{1}H-^{13}C$ HSQC spectra of the intact mitochondria at the beginning (0.5 h after extraction) and at the end (12.5 h after extraction) of the observation. To ensure the reliability of cyt c resonances observed in mitochondria, HSQC spectra of cyt c in different contents of CL liposome and H_2O_2 were also obtained (Figures S13 and S14).

During the experiment, it was observed that only one set of resonances from cyt c that bind to IMM was detected in the initial spectrum. This finding suggests that the majority of cyt c in normal mitochondria binds to the IMM. However, in the final spectrum, another set of signals appears (labeled by asterisks), indicating that some cyt c was released from the IMM. This result was further confirmed by the inspection of the time-dependent spectra of cyt c (Figure 4B). The resonances assigned to the bound cyt c in CL gradually decreased over time, while the corresponding signals from free cyt c increased progressively, illustrating the translocation of cyt c. Notably, no signals of cyt c were detected in the supernatant extracted from the NMR sample at the end of the experiment, indicating that the released cyt c was located in the IMS but did not leak into the solvent. Cyt c is widely recognized as an electron carrier in the electron transport chain that triggers the production of ROS, such as O_2^- or H_2O_2. Isolated mitochondria typically experience oxidative stress over time,[64] raising internal ROS levels,[65,66] and leading to an increase in the release of cyt c. We hypothesize that the new set of NMR signals with gradually enhanced intensities may be attributed to the accumulation of ROS in oxidatively stressed mitochondria. To verify this, we measured peak intensities of each time-dependent spectrum of both free and bound cyt c and compared them with changes in internal ROS in mitochondria (Figure 4C,D). According to the results, the trend of the increase in free cyt c over time is consistent with that of internal ROS in mitochondria. This suggests a positive correlation between the translocation of cyte c and oxidative stress in mitochondria.

The increase in the level of ROS in the mitochondria is possible because of hypoxia. Under hypoxic conditions, cellular metabolism is incomplete, resulting in the rapid production of ROS.[67] Therefore, we quantitatively detected the OCR of

https://doi.org/10.1021/jacs.3c10216
J. Am. Chem. Soc. 2024, 146, 4455−4466

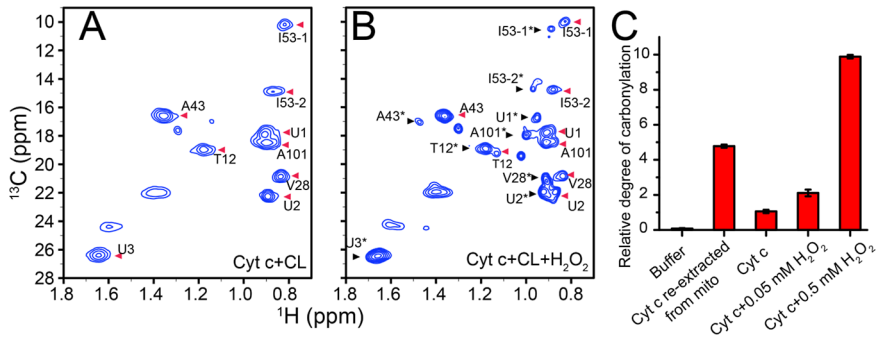

Figure 5. Release and carbonylation of cyt c under oxidative conditions. (A,B) $^{1}H-^{13}C$ HSQC spectra of 0.1 mM cyt c mixed with 0.5 mM CL liposomes in the absence and presence of 0.5 mM H_2O_2, respectively. (C) Carbonylation of 0.01 mM cyt c under various treatments.

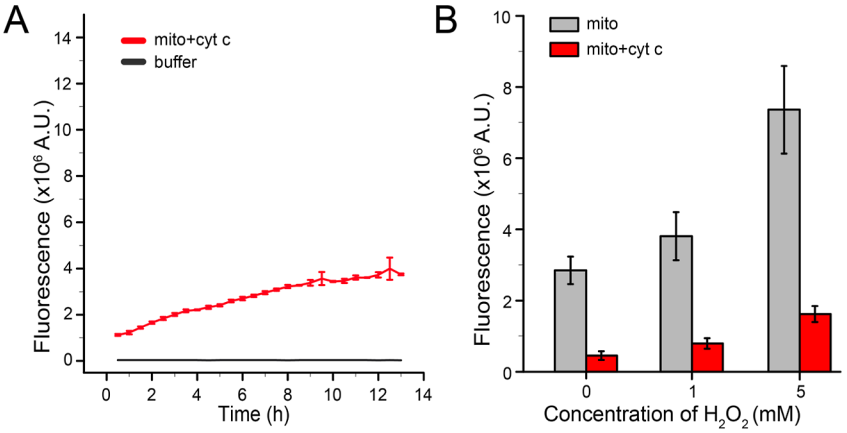

Figure 6. Detection of internal ROS in mitochondria using the DCFH-DA fluorescence probe. (A) Changes in the ROS levels in mitochondria over time after electroporation of cyt c. (B) Comparison of the ROS levels in living mitochondria extracted from yeast in the absence and presence of H_2O_2 within 2 h.

mitochondria at different time points, as shown in Figure 4E. The OCR of mitochondria gradually weakened over time, which corresponds to the increasing trend of ROS in mitochondria. The result further indicates that mitochondria undergo oxidative stress after separation from yeast.

According to this situation, we tested the functionality and activity of separated mitochondria during a real-time observation period. MTT is a specific reagent used to detect mitochondrial functionality.[45] From Figure 4F, it can be seen that more than 85% of mitochondria were still well functional over 12.5 h. The sustained activity and integrity of mitochondria were further confirmed by using Janus green B and MitoTracker Red CMXRos staining (Figure S15). In general, these results suggest that mitochondria were consistently active and intact throughout the whole process of the real-time experiments.

Oxidative Modification and Release of Cyt c in the CL Liposomes. To provide further evidence that the release of cyt c from the IMM is triggered by internal ROS, a comparative experiment was conducted. Two NMR spectra of cyt c in CL liposomes with and without H_2O_2 were acquired and compared to each other. The results, presented in Figure 5A,B, show that in the absence of H_2O_2, the spectra of cyt c interacting with CL were similar to those of the bound cyt c in mitochondria. However, in the presence of 0.5 mM H_2O_2 (a concentration previously used in assays [17]), some new signals appeared, similar to the free cyt c observed in mitochondria. These findings confirm that oxidative stress can cause the release of cyt c from IMM.

Mitochondria have been reported as the primary sources of ROS in most aerobic mammalian cells. This ROS production by mitochondria plays a crucial role in retrograde redox signaling from the organelle, cytosol to the nucleus.[68] As a result, translocation and conformational changes of cyt c in conjunction with ROS production indicate that cyt c is suitable for sensing and signaling oxidative stress. It is not surprising that cyt c has been shown to act as an antioxidant by regulating the generation and elimination of O_2^- and H_2O_2 within mitochondria.[69]

Some studies have demonstrated that cyt c can undergo carbonylation modification in a dilute solution upon exposure to ROS, mainly on lysine residues. These lysine residues are crucial for the electrostatic interaction of cyt c with CL.[70] Oxidative modification of cyt c weakens this interaction, as carbonylation changes the positively charged side chain to an uncharged aldehyde.[62] To determine if cyt c undergoes oxidative modification in mitochondria, we detected carbonylation of cyt c extracted from mitochondria and in a dilute solution under oxidative conditions. H_2O_2, a high-content ROS that accumulates during oxidative stress, was used as a positive control to verify oxidative modification. The use of 2,4 dinitrophenylhydrazine (DNPH) has been established for detecting protein carbonylation.[71] DNPH selectively binds to the carbonyl groups of proteins, producing distinct absorption at 370 nm in the UV−visible spectrum. To enhance sensitivity, additional cyt c was introduced into mitochondria *via* electroporation to match the NMR sample conditions. The mitochondria containing transferred cyt c were centrifuged

https://doi.org/10.1021/jacs.3c10216
J. Am. Chem. Soc. 2024, 146, 4455−4466

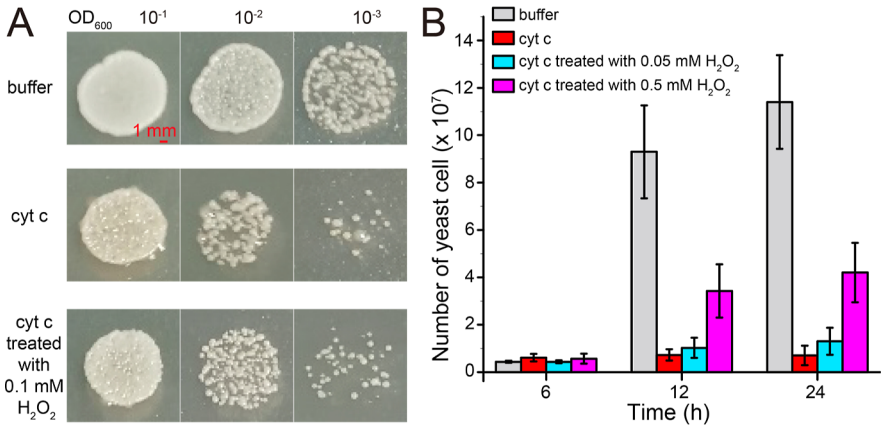

Figure 7. Growth of the yeast cells, comparing those transfected with or without cyt c. (A) Growth of the yeast cells transfected without cyt c and with normal and oxidized cyt c. (B) Growth of the yeast cells transfected with cyt c (0.5 mM), which was oxidized using various concentrations of H_2O_2.

multiple times to remove any surface attached to cyt c, incubated at room temperature for 12 h, and then lysed to extract the internal cyt c.

The difference in carbonylation levels of cyt c under various conditions is depicted in Figure 5C. The carbonyl content of cyt c in solution increased gradually with the addition of H_2O_2, indicating that carbonylation occurs when cyt c is exposed to H_2O_2. Comparatively, cyt c purified from mitochondria incubated at room temperature for 12 h also displayed a high degree of carbonylation. These results demonstrate that carbonylation modifications occur on cyt c in mitochondria. It is noteworthy that carbonylation exists in cyt c even in the absence of H_2O_2, which is reasonable since cyt c is easily oxidized when exposed to air.[72]

Cyt c Scavenges ROS in Mitochondria during Oxidative Stress. ROS has a dual nature, serving as both an antimicrobial agent and a participant in pathways that regulate programmed cell death, including apoptosis and autophagy.[68] Consequently, it is essential to understand the impact of cyt c on ROS. We monitored internal mitochondrial ROS levels over time after electroporation with 0.5 mM cyt c (Figure 6A). In contrast to normal mitochondria without cyt c electroporation (Figure 4D), the internal ROS level in mitochondria with extra cyt c increased significantly more slowly, and the highest ROS level was less than one-third of that in normal mitochondria during the same detection period. Furthermore, static levels of internal ROS in mitochondria at different H_2O_2 concentrations indicate that cyt c can act as a ROS scavenger in mitochondria, dramatically reducing ROS levels (Figure 6B). Since H_2O_2 is a known inducer of apoptosis in yeast,[73] the results imply that cyt c may play a crucial role in antiapoptosis in mitochondria by eliminating excess ROS, while translocation and oxidative modification are involved.

Oxidatively Modified Cyt c Has Reduced Impacts on Cell Apoptosis. Although cyt c in mitochondria was not released for a relatively short period (within 2 h), when mitochondria were extracted and left at room temperature for over 12 h, we detected the leaking cyt c in the supernatant (Figure S16). This indicates that as oxidative stress keeps elevating, the mitochondria are failing to resist high concentrations of ROS and releasing cyt c.

It was known that cyt c dropped into the cytoplasm typically triggers apoptosis by initiating the activation cascade of caspases. Given our evidence suggesting that a portion of cyt c is subject to oxidative modification in the presence of high levels of H_2O_2, it raises the question of whether these oxidative modifications, originating from the IMM, retain the same apoptotic effects upon reaching the cytoplasm.

To evaluate the effects of oxidatively modified cyt c on cell apoptosis, we monitored the growth of yeast cells transfected with and without cyt c (Figure 7A). As expected, yeast cells transfected with normal cyt c showed observably reduced growth.[74] While those transfected with cyt c treated with 0.1 mM H_2O_2 had a weaker suppression of growth. Furthermore, the higher the concentrations of H_2O_2 treated with cyt c, the lighter the suppression of cell growth after transfection (Figure 7B). This outcome presents the probability that oxidative modification may have a protective effect on cyt c-induced apoptosis.

Yeast cells are useful model organisms for studying apoptosis and undergo apoptosis under exposure to various external stimuli.[73] The release of cyt c from mitochondria initiates apoptosis by interacting with apoptotic peptidase activating factor 1 (Apaf1) and activating caspase *via* some positively charged residues like lysine on the surface of cyt c.[75,76] Therefore, combined with our discoveries, it is reasonable to propose the hypothesis that oxidative modification reduces the impact of cyt c on apoptosis by altering the charge of these positively charged residues, potentially weakening the electrostatic interaction of cyt c with Apaf1.

■ CONCLUSIONS

Proteins are essential for regulating and performing various physiological functions in intact organisms. Determining the structures of proteins under physiological conditions provides accurate insights into the elucidation of protein functional mechanisms. However, it poses significant challenges due to the complex and dynamic nature of proteins within the cellular environment.

This study used NMR to investigate the conformation and translocation of cyt c, a multifunctional protein, in mitochondria. By observing methyl groups in the protein, $^{1}H-^{13}C$ NMR spectroscopy was able to probe cyt c in intact mitochondria directly, in real-time and without overexpression. This was feasible due to the detectable concentration of cyt c in mitochondria and the high NMR sensitivity of methyl groups.

It has been discovered that cyt c in intact mitochondria, unlike in solution, is partially unfolded and mainly binds to the

https://doi.org/10.1021/jacs.3c10216
J. Am. Chem. Soc. 2024, 146, 4455−4466

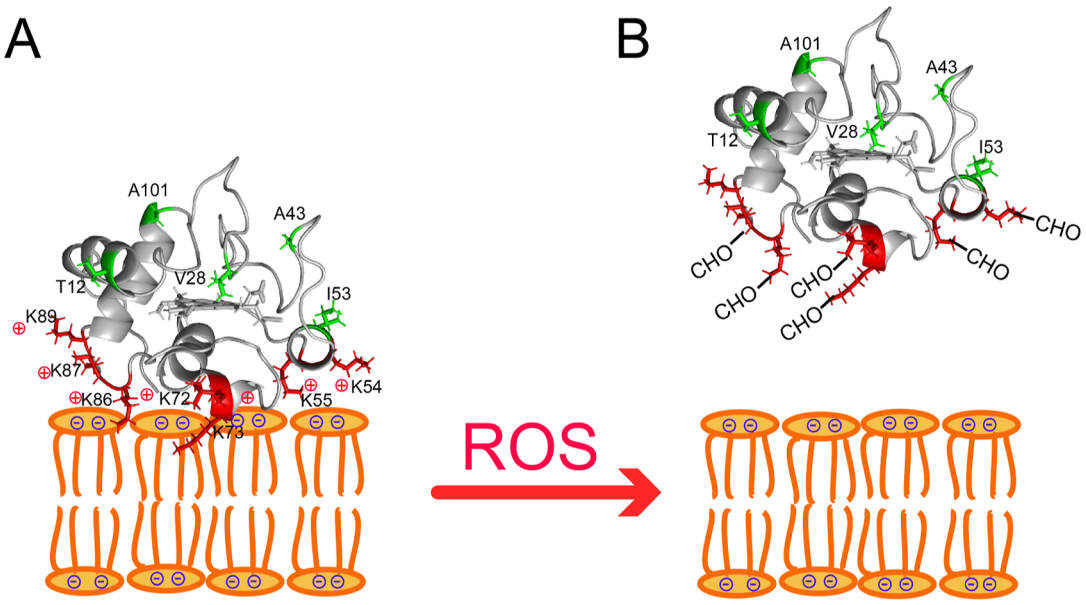

Figure 8. Diagram of the location and modification of cyt c in mitochondria during oxidative stress. (A) Under normal conditions, cyt c binds to the IMM through electrostatic interactions. (B) Under oxidation stress, increased ROS results in carbonyl modification of the protein, causing its release from the IMM to the IMS.

IMM through electrostatic interactions (Figure 8A). This conformation exposes the heme of the protein, leading to higher peroxidase activity and efficient scavenging of ROS.[19,69] Real-time NMR spectra revealed that cyt c in mitochondria gradually changed location and was prone to being oxidatively modified by increased ROS,[68] which induced carbonyl modifications on lysine residues and ruptures in the interactions between cyt c and CL in the mitochondrial membrane (Figure 8B). The modified cyt c was released from the membrane and significantly counteracted the effect brought by the original cyt c form on cell growth. These findings suggest that yeast cyt c is a highly efficient ROS scavenger in mitochondria,[19,69] and oxidative modification may serve a protective role against oxidative stress, indicating the importance of cyt c translocation and oxidative modification in regulating ROS in mitochondria.

■ ASSOCIATED CONTENT

Supporting Information

The Supporting Information is available free of charge at https://pubs.acs.org/doi/10.1021/jacs.3c10216.

NMR spectra, EPR spectra, UV−visible spectra, and mitochondrial staining data (PDF)

■ AUTHOR INFORMATION

Corresponding Authors

Maili Liu − *State Key Laboratory of Magnetic Resonance and Atomic and Molecular Physics, National Center for Magnetic Resonance in Wuhan, Wuhan Institute of Physics and Mathematics, Innovation Academy for Precision Measurement of Science and Technology, Chinese Academy of Sciences, Wuhan 430071, People's Republic of China; University of Chinese Academy of Sciences, Beijing 100049, People's Republic of China; Wuhan National Laboratory for Optoelectronics, Huazhong University of Science and Technology, Wuhan 430071, People's Republic of China; Optics Valley Laboratory, Wuhan 430074, People's Republic of China;* orcid.org/0000-0002-9359-915X; Email: ml.liu@wipm.ac.cn

Xu Zhang − *State Key Laboratory of Magnetic Resonance and Atomic and Molecular Physics, National Center for Magnetic Resonance in Wuhan, Wuhan Institute of Physics and Mathematics, Innovation Academy for Precision Measurement of Science and Technology, Chinese Academy of Sciences, Wuhan 430071, People's Republic of China; University of Chinese Academy of Sciences, Beijing 100049, People's Republic of China; Wuhan National Laboratory for Optoelectronics, Huazhong University of Science and Technology, Wuhan 430071, People's Republic of China; Optics Valley Laboratory, Wuhan 430074, People's Republic of China;* orcid.org/0000-0003-2481-946X; Email: zhangxu@wipm.ac.cn

Authors

Jianhua Zhan − *State Key Laboratory of Magnetic Resonance and Atomic and Molecular Physics, National Center for Magnetic Resonance in Wuhan, Wuhan Institute of Physics and Mathematics, Innovation Academy for Precision Measurement of Science and Technology, Chinese Academy of Sciences, Wuhan 430071, People's Republic of China; University of Chinese Academy of Sciences, Beijing 100049, People's Republic of China*

Danyun Zeng − *State Key Laboratory of Magnetic Resonance and Atomic and Molecular Physics, National Center for Magnetic Resonance in Wuhan, Wuhan Institute of Physics and Mathematics, Innovation Academy for Precision Measurement of Science and Technology, Chinese Academy of Sciences, Wuhan 430071, People's Republic of China; University of Chinese Academy of Sciences, Beijing 100049, People's Republic of China*

Xiong Xiao − *State Key Laboratory of Magnetic Resonance and Atomic and Molecular Physics, National Center for Magnetic Resonance in Wuhan, Wuhan Institute of Physics and Mathematics, Innovation Academy for Precision Measurement of Science and Technology, Chinese Academy of*

https://doi.org/10.1021/jacs.3c10216
J. Am. Chem. Soc. 2024, 146, 4455−4466

Sciences, Wuhan 430071, People's Republic of China; University of Chinese Academy of Sciences, Beijing 100049, People's Republic of China

Zhongpei Fang − *State Key Laboratory of Magnetic Resonance and Atomic and Molecular Physics, National Center for Magnetic Resonance in Wuhan, Wuhan Institute of Physics and Mathematics, Innovation Academy for Precision Measurement of Science and Technology, Chinese Academy of Sciences, Wuhan 430071, People's Republic of China; University of Chinese Academy of Sciences, Beijing 100049, People's Republic of China*

Tao Huang − *State Key Laboratory of Magnetic Resonance and Atomic and Molecular Physics, National Center for Magnetic Resonance in Wuhan, Wuhan Institute of Physics and Mathematics, Innovation Academy for Precision Measurement of Science and Technology, Chinese Academy of Sciences, Wuhan 430071, People's Republic of China; University of Chinese Academy of Sciences, Beijing 100049, People's Republic of China*

Beibei Zhao − *State Key Laboratory of Magnetic Resonance and Atomic and Molecular Physics, National Center for Magnetic Resonance in Wuhan, Wuhan Institute of Physics and Mathematics, Innovation Academy for Precision Measurement of Science and Technology, Chinese Academy of Sciences, Wuhan 430071, People's Republic of China; University of Chinese Academy of Sciences, Beijing 100049, People's Republic of China*

Qinjun Zhu − *State Key Laboratory of Magnetic Resonance and Atomic and Molecular Physics, National Center for Magnetic Resonance in Wuhan, Wuhan Institute of Physics and Mathematics, Innovation Academy for Precision Measurement of Science and Technology, Chinese Academy of Sciences, Wuhan 430071, People's Republic of China; University of Chinese Academy of Sciences, Beijing 100049, People's Republic of China*

Caixiang Liu − *State Key Laboratory of Magnetic Resonance and Atomic and Molecular Physics, National Center for Magnetic Resonance in Wuhan, Wuhan Institute of Physics and Mathematics, Innovation Academy for Precision Measurement of Science and Technology, Chinese Academy of Sciences, Wuhan 430071, People's Republic of China; University of Chinese Academy of Sciences, Beijing 100049, People's Republic of China*

Bin Jiang − *State Key Laboratory of Magnetic Resonance and Atomic and Molecular Physics, National Center for Magnetic Resonance in Wuhan, Wuhan Institute of Physics and Mathematics, Innovation Academy for Precision Measurement of Science and Technology, Chinese Academy of Sciences, Wuhan 430071, People's Republic of China; University of Chinese Academy of Sciences, Beijing 100049, People's Republic of China; Wuhan National Laboratory for Optoelectronics, Huazhong University of Science and Technology, Wuhan 430071, People's Republic of China; Optics Valley Laboratory, Wuhan 430074, People's Republic of China*

Xin Zhou − *State Key Laboratory of Magnetic Resonance and Atomic and Molecular Physics, National Center for Magnetic Resonance in Wuhan, Wuhan Institute of Physics and Mathematics, Innovation Academy for Precision Measurement of Science and Technology, Chinese Academy of Sciences, Wuhan 430071, People's Republic of China; University of Chinese Academy of Sciences, Beijing 100049, People's Republic of China; Wuhan National Laboratory for Optoelectronics, Huazhong University of Science and Technology, Wuhan 430071, People's Republic of China; Optics Valley Laboratory, Wuhan 430074, People's Republic of China;* orcid.org/0000-0002-5580-7907

Conggang Li − *State Key Laboratory of Magnetic Resonance and Atomic and Molecular Physics, National Center for Magnetic Resonance in Wuhan, Wuhan Institute of Physics and Mathematics, Innovation Academy for Precision Measurement of Science and Technology, Chinese Academy of Sciences, Wuhan 430071, People's Republic of China; University of Chinese Academy of Sciences, Beijing 100049, People's Republic of China; Wuhan National Laboratory for Optoelectronics, Huazhong University of Science and Technology, Wuhan 430071, People's Republic of China;* orcid.org/0000-0002-5798-1722

Lichun He − *State Key Laboratory of Magnetic Resonance and Atomic and Molecular Physics, National Center for Magnetic Resonance in Wuhan, Wuhan Institute of Physics and Mathematics, Innovation Academy for Precision Measurement of Science and Technology, Chinese Academy of Sciences, Wuhan 430071, People's Republic of China; University of Chinese Academy of Sciences, Beijing 100049, People's Republic of China*

Daiwen Yang − *Department of Biological Sciences, National University of Singapore, Singapore 117543, Singapore;* orcid.org/0000-0002-6804-0071

Complete contact information is available at: https://pubs.acs.org/10.1021/jacs.3c10216

Notes

The authors declare no competing financial interest.

■ ACKNOWLEDGMENTS

We would like to thank Professor Haijun Yang at Tsinghua University for his kind help in the EPR experiments. This work was supported by the National Key R&D Program of China (2018YFE0202300, 2018YFA0704002, and 2017YFA0505400), the National Natural Science Foundation of China (21974149, 22174152, 21505153, 21475146, 21991081, 21921004, and 21735007), the Hubei Provincial Natural Science Foundation of China (2023AFA041), and the Strategic Priority Research Program of the Chinese Academy of Sciences (XDB0540000).

■ REFERENCES

(1) Alvarez-Paggi, D.; Hannibal, L.; Castro, M. A.; Oviedo-Rouco, S.; Demicheli, V.; Tortora, V.; Tomasina, F.; Radi, R.; Murgida, D. H. Multifunctional Cytochrome c: Learning New Tricks from an Old Dog. *Chem. Rev.* **2017**, *117* (21), 13382−13460.

(2) Saraste, M. Oxidative phosphorylation at the fin de siecle. *Science* **1999**, *283* (5407), 1488−1493.

(3) Atlante, A.; Calissano, P.; Bobba, A.; Azzariti, A.; Marra, E.; Passarella, S. Cytochrome c is released from mitochondria in a reactive oxygen species (ROS)-dependent fashion and can operate as a ROS scavenger and as a respiratory substrate in cerebellar neurons undergoing excitotoxic death. *J. Biol. Chem.* **2000**, *275* (47), 37159−37166.

(4) Xu, T.; Yang, Q.; Wang, B.; Wang, W.; Li, J.; Ma, Y.; Gao, X. Cytochrome c injection induced embryo loss. *Drug Chem. Toxicol.* **2021**, *44* (5), 544−549.

(5) Gogvadze, V.; Orrenius, S.; Zhivotovsky, B. Multiple pathways of cytochrome c release from mitochondria in apoptosis. *BBA-Bioenergetics.* **2006**, *1757* (5−6), 639−647.

(6) Ow, Y. L. P.; Green, D. R.; Hao, Z.; Mak, T. W. Cytochrome c: functions beyond respiration. *Nat. Rev. Mol. Cell Biol.* **2008**, *9* (7), 532−542.
(7) Hannibal, L.; Tomasina, F.; Capdevila, D. A.; Demicheli, V.; Tortora, V.; Alvarez-Paggi, D.; Jemmerson, R.; Murgida, D. H.; Radi, R. Alternative Conformations of Cytochrome c: Structure, Function, and Detection. *Biochemistry* **2016**, *55* (3), 407−428.
(8) Baistrocchi, P.; Banci, L.; Bertini, I.; Turano, P.; Bren, K. L.; Gray, H. B. Three-dimensional solution structure of Saccharomyces cerevisiae reduced iso-1-cytochrome c. *Biochemistry* **1996**, *35* (43), 13788−13796.
(9) Banci, L.; Bertini, I.; Bren, K. L.; Gray, H. B.; Sompornpisut, P.; Turano, P. Solution structure of oxidized Saccharomyces cerevisiae iso-1-cytochrome c. *Biochemistry* **1997**, *36* (29), 8992−9001.
(10) Zaidi, S.; Hassan, M. I.; Islam, A.; Ahmad, F. The role of key residues in structure, function, and stability of cytochrome-c. *Cell. Mol. Life Sci.* **2014**, *71* (2), 229−255.
(11) Nelson, C. J.; Bowler, B. E. pH dependence of formation of a partially unfolded state of a Lys 73 -> His variant of iso-1-cytochrome c: implications for the alkaline conformational transition of cytochrome c. *Biochemistry* **2000**, *39* (44), 13584−13594.
(12) Pascher, T. Temperature and driving force dependence of the folding rate of reduced horse heart cytochrome c. *Biochemistry* **2001**, *40* (19), 5812−5820.
(13) Prabhakaran, M.; Gursahani, S. H.; Verma, C. S.; Garduno-Juarez, R.; Renugopalakrishnan, V. Cytochrome c: the effect of temperature and pressure from molecular dynamics simulations. *J. Phys. Chem. Solids* **2004**, *65* (8−9), 1615−1622.
(14) Brieger, K.; Schiavone, S.; Miller, J., Jr.; Krause, K.-H. Reactive oxygen species: from health to disease. *Swiss Med. Wkly.* **2012**, *142*, w13659.
(15) D'Autreaux, B.; Toledano, M. B. ROS as signalling molecules: mechanisms that generate specificity in ROS homeostasis. *Nat. Rev. Mol. Cell Biol.* **2007**, *8* (10), 813−824.
(16) Hu, J.; Dong, L.; Outten, C. E. The redox environment in the mitochondrial intermembrane space is maintained separately from the cytosol and matrix. *J. Biol. Chem.* **2008**, *283* (43), 29126−29134.
(17) Yin, V.; Shaw, G. S.; Konermann, L. Cytochrome c as a Peroxidase: Activation of the Precatalytic Native State by H2O2-Induced Covalent Modifications. *J. Am. Chem. Soc.* **2017**, *139* (44), 15701−15709.
(18) Hanske, J.; Toffey, J. R.; Morenz, A. M.; Bonilla, A. J.; Schiavoni, K. H.; Pletneva, E. V. Conformational properties of cardiolipin-bound cytochrome c. *Proc. Natl. Acad. Sci. U.S.A.* **2012**, *109* (1), 125−130.
(19) Muenzner, J.; Toffey, J. R.; Hong, Y. N.; Pletneva, E. V. Becoming a Peroxidase: Cardiolipin-Induced Unfolding of Cytochrome c. *J. Phys. Chem. B* **2013**, *117* (42), 12878−12886.
(20) Brazhe, N. A.; Evlyukhin, A. B.; Goodilin, E. A.; Semenova, A. A.; Novikov, S. M.; Bozhevolnyi, S. I.; Chichkov, B. N.; Sarycheva, A. S.; Baizhumanov, A. A.; Nikelshparg, E. I.; Deev, L. I.; Maksimov, E. G.; Maksimov, G. V.; Sosnovtseva, O. Probing cytochrome c in living mitochondria with surface-enhanced Raman spectroscopy. *Sci. Rep.* **2015**, *5*, 13793.
(21) Pessoa, J. Live-cell visualization of cytochrome c: a tool to explore apoptosis. *Biochem. Soc. Trans.* **2021**, *49* (6), 2903−2915.
(22) Liu, J.; Wang, Z.-Q.; Mao, G.-J.; Jiang, W.-L.; Tan, M.; Xu, F.; Li, C.-Y. A near-infrared fluorescent probe with large Stokes shift for imaging Cys in tumor mice. *Anal. Chim. Acta* **2021**, *1171*, 338655.
(23) Antholine, W. E.; Vasquez-Vivar, J.; Quirk, B. J.; Whelan, H. T.; Wu, P. K.; Park, J. I.; Myers, C. R. Treatment of Cells and Tissues with Chromate Maximizes Mitochondrial 2Fe2S EPR Signals. *Int. J. Mol. Sci.* **2019**, *20* (5), 1143.
(24) Bonucci, A.; Ouari, O.; Guigliarelli, B.; Belle, V.; Mileo, E. In-Cell EPR: Progress towards Structural Studies Inside Cells. *ChemBioChem* **2020**, *21* (4), 451−460.
(25) Kucher, S.; Korneev, S.; Klare, J. P.; Klose, D.; Steinhoff, H. J. In cell Gd^{3+}-based site-directed spin labeling and EPR spectroscopy of eGFP. *Phys. Chem. Chem. Phys.* **2020**, *22* (24), 13358−13362.
(26) Theillet, F. X.; Luchinat, E. In-cell NMR: Why and how? *Prog. Nucl. Magn. Reson. Spectrosc.* **2022**, *132*−*133*, 1−112.
(27) Luchinat, E.; Cremonini, M.; Banci, L. Radio Signals from Live Cells: The Coming of Age of In-Cell Solution NMR. *Chem. Rev.* **2022**, *122* (10), 9267−9306.
(28) Theillet, F. X. In-Cell Structural Biology by NMR: The Benefits of the Atomic Scale. *Chem. Rev.* **2022**, *122* (10), 9497−9570.
(29) Yamaoki, Y.; Kiyoishi, A.; Miyake, M.; Kano, F.; Murata, M.; Nagata, T.; Katahira, M. The first successful observation of in-cell NMR signals of DNA and RNA in living human cells. *Phys. Chem. Chem. Phys.* **2018**, *20* (5), 2982−2985.
(30) Gowda, G. A. N. Profiling Redox and Energy Coenzymes in Whole Blood, Tissue and Cells Using NMR Spectroscopy. *Metabolites* **2018**, *8* (2), 32.
(31) Lipok, J.; Wieczorek, D.; Jewginski, M.; Kafarski, P. Prospects of in vivo 31P NMR method in glyphosate degradation studies in whole cell system. *Enzyme Microb. Technol.* **2009**, *44* (1), 11−16.
(32) Barbieri, L.; Luchinat, E.; Banci, L. Structural insights of proteins in sub-cellular compartments: In-mitochondria NMR. *BBA-Mol. Cell Res.* **2014**, *1843* (11), 2492−2496.
(33) Amor, I. Y. H.; Smaoui, K.; Chaabène, I.; Mabrouk, I.; Djemal, L.; Elleuch, H.; Allouche, M.; Mokdad-Gargouri, R.; Gargouri, A. Human p53 induces cell death and downregulates thioredoxin expression in Saccharomyces cerevisiae. *FEMS Yeast Res.* **2008**, *8* (8), 1254−1262.
(34) Sialana, F. J.; Wang, A. L.; Fazari, B.; Kristofova, M.; Smidak, R.; Trossbach, S. V.; Korth, C.; Huston, J. P.; de Souza Silva, M. A.; Lubec, G. Quantitative Proteomics of Synaptosomal Fractions in a Rat Overexpressing Human DISC1 Gene Indicates Profound Synaptic Dysregulation in the Dorsal Striatum. *Front. Mol. Neurosci.* **2018**, *11*, 26−37.
(35) Namba, S.; Kato, H.; Shigenobu, S.; Makino, T.; Moriya, H. Massive expression of cysteine-containing proteins causes abnormal elongation of yeast cells by perturbing the proteasome. *G3: Genes, Genomes, Genet.* **2022**, *12* (6), jkac106.
(36) Pastore, A.; Temussi, P. A. The Emperor's new clothes: Myths and truths of in-cell NMR. *Arch. Biochem. Biophys.* **2017**, *628*, 114−122.
(37) Korshunov, S. S.; Krasnikov, B. F.; Pereverzev, M. O.; Skulachev, V. P. The antioxidant functions of cytochrome c. *Febs Lett.* **1999**, *462* (1−2), 192−198.
(38) Forman, H. J.; Azzi, A. On the virtual existence of superoxide anions in mitochondria: Thoughts regarding its role in pathophysiology. *FASEB J.* **1997**, *11* (5), 374−375.
(39) Wieckowski, M. R.; Giorgi, C.; Lebiedzinska, M.; Duszynski, J.; Pinton, P. Isolation of mitochondria-associated membranes and mitochondria from animal tissues and cells. *Nat. Protoc.* **2009**, *4* (11), 1582−1590.
(40) Nishimura, N.; Yano, M. Separation of the Inner and Outer Mitochondrial Membrane in HeLa Cells. *Bio-Protoc.* **2014**, *4* (22), 1−4.
(41) Brustovetsky, N.; Jemmerson, R.; Dubinsky, J. M. Calcium-induced Cytochrome c release from rat brain mitochondria is altered by digitonin. *Neurosci. Lett.* **2002**, *332* (2), 91−94.
(42) Pandiscia, L. A.; Schweitzer-Stenner, R. Salt as a catalyst in the mitochondria: returning cytochrome c to its native state after it misfolds on the surface of cardiolipin containing membranes. *Chem. Commun.* **2014**, *50* (28), 3674−3676.
(43) Szabo, C. M.; Sanders, L. K.; Le, H. C.; Chien, E. Y. T.; Oldfield, E. Expression of doubly labeled Saccharomyces cerevisiae iso-1 ferricytochrome c and ^{1}H, ^{13}C and ^{15}N chemical shift assignments by multidimensional NMR. *Febs Lett.* **2000**, *482* (1−2), 25−30.
(44) Zhu, J. Y.; Jiang, M. W.; Ma, H.; Zhang, H. J.; Cheng, W. N.; Li, J. B.; Cai, L. J.; Han, X. X.; Zhao, B. Redox-State-Mediated Regulation of Cytochrome c Release in Apoptosis Revealed by Surface-Enhanced Raman Scattering on Nickel Substrates. *Angew. Chem., Int. Ed.* **2019**, *58* (46), 16499−16503.

https://doi.org/10.1021/jacs.3c10216
J. Am. Chem. Soc. 2024, 146, 4455−4466

(45) Slater, T. F.; Sawyer, B.; Sträuli, U. Studies on succinate-tetrazolium reductase systems. *Biochim. Biophys. Acta* **1963**, *77*, 383−393.
(46) Xu, W. J.; Wen, H.; Kim, H. S.; Ko, Y. J.; Dong, S. M.; Park, I. S.; Yook, J. I.; Park, S. Observation of acetyl phosphate formation in mammalian mitochondria using real-time in-organelle NMR metabolomics. *Proc. Natl. Acad. Sci. U.S.A.* **2018**, *115* (16), 4152−4157.
(47) Brazhe, N. A.; Nikelshparg, E. I.; Baizhumanov, A. A.; Grivennikova, V. G.; Semenova, A. A.; Novikov, S. M.; Volkov, V. S.; Arsenin, A. V.; Yakubovsky, D. I.; Evlyukhin, A. B.; Bochkova, Z. V.; Goodilin, E. A.; Maksimov, G. V.; Sosnovtseva, O.; Rubin, A. B. SERS uncovers the link between conformation of cytochrome c heme and mitochondrial membrane potential. *Free Radical Biol. Med.* **2023**, *196*, 133−144.
(48) Gott, J. M.; Naegele, G. M.; Howell, S. J. Electroporation of DNA into Physarum polycephalum Mitochondria: Effects on Transcription and RNA Editing in Isolated Organelles. *Genes* **2016**, *7* (12), 128−141.
(49) Danielsson, J.; Mu, X.; Lang, L.; Wang, H.; Binolfi, A.; Theillet, F.-X.; Bekei, B.; Logan, D. T.; Selenko, P.; Wennerstrom, H.; Oliveberg, M. Thermodynamics of protein destabilization in live cells. *Proc. Natl. Acad. Sci. U.S.A.* **2015**, *112* (40), 12402−12407.
(50) Jagger, A. M.; Waudby, C. A.; Irving, J. A.; Christodoulou, J.; Lomas, D. A. High-resolution ex vivo NMR spectroscopy of human Z alpha(1)-antitrypsin. *Nat. Commun.* **2020**, *11*, 6371.
(51) Jin, X.; Kang, S.; Tanaka, S.; Park, S. Monitoring the Glutathione Redox Reaction in Living Human Cells by Combining Metabolic Labeling with Heteronuclear NMR. *Angew. Chem., Int. Ed.* **2016**, *55* (28), 7939−7942.
(52) Ascenzi, P.; Coletta, M.; Wilson, M. T.; Fiorucci, L.; Marino, M.; Polticelli, F.; Sinibaldi, F.; Santucci, R. Cardiolipin-Cytochrome c Complex: Switching Cytochrome c from an Electron-Transfer Shuttle to a Myoglobin- and a Peroxidase-like Heme-protein. *IUBMB Life* **2015**, *67* (2), 98−109.
(53) Zhan, J.; Zhang, G.; Chai, X.; Zhu, Q.; Sun, P.; Jiang, B.; Zhou, X.; Zhang, X.; Liu, M. NMR Reveals the Conformational Changes of Cytochrome C upon Interaction with Cardiolipin. *Life (Basel, Switzerland)* **2021**, *11* (10), 1031.
(54) Fang, Z.; Sun, P.; Wang, Q.; Zhang, L.; Liu, M.; Zhang, X. Conformational change of wild type cytochrome c characterized by NMR spectroscopy at natural isotropic abundance. *Chinese J. of Magn Reson* **2019**, *36* (4), 481−489.
(55) Kofuku, Y.; Ueda, T.; Okude, J.; Shiraishi, Y.; Kondo, K.; Maeda, M.; Tsujishita, H.; Shimada, I. Efficacy of the β_2-adrenergic receptor is determined by conformational equilibrium in the transmembrane region. *Nat. Commun.* **2012**, *3* (1), 1045.
(56) Amacher, J. F.; Zhong, F.; Lisi, G. P.; Zhu, M. Q.; Alden, S. L.; Hoke, K. R.; Madden, D. R.; Pletneva, E. V. A Compact Structure of Cytochrome c Trapped in a Lysine-Ligated State: Loop Refolding and Functional Implications of a Conformational Switch. *J. Am. Chem. Soc.* **2015**, *137* (26), 8435−8449.
(57) Srour, B.; Stampraad, M. J. F.; Hagen, W. R.; Hagedoorn, P.-L. Refolding kinetics of cytochrome c studied with microsecond timescale continuous-flow UV-vis spectroscopy and rapid freeze-quench EPR. *J. Inorg. Biochem.* **2018**, *184*, 42−49.
(58) Silkstone, G. G.; Cooper, C. E.; Svistunenko, D.; Wilson, M. T. EPR and optical spectroscopic studies of Met80X mutants of yeast ferricytochrome c. models for intermediates in the alkaline transition. *J. Am. Chem. Soc.* **2005**, *127* (1), 92−99.
(59) Zucchi, M. R.; Nascimento, O. R.; Faljoni-Alario, A.; Prieto, T.; Nantes, I. L. Modulation of cytochrome c spin states by lipid acyl chains: a continuous-wave electron paramagnetic resonance (CW-EPR) study of haem iron. *Biochem. J.* **2003**, *370*, 671−678.
(60) Nantes, I. L.; Zucchi, M. R.; Nascimento, O. R.; Faljoni-Alario, A. Effect of Heme Iron Valence State on the Conformation of Cytochrome c and Its Association with Membrane Interfaces. *J. Biol. Chem.* **2001**, *276* (1), 153−158.
(61) Yin, V.; Mian, S. H.; Konermann, L. Lysine carbonylation is a previously unrecognized contributor to peroxidase activation of cytochrome c by chloramine-T. *Chem. Sci.* **2019**, *10* (8), 2349−2359.
(62) Barayeu, U.; Lange, M.; Méndez, L.; Arnhold, J.; Shadyro, O. I.; Fedorova, M.; Flemmig, J. Cytochrome c auto-catalyzed carbonylation in the presence of hydrogen peroxide and cardiolipins. *J. Biol. Chem.* **2019**, *294* (6), 1816−1830.
(63) Sinibaldi, F.; Milazzo, L.; Howes, B. D.; Piro, M. C.; Fiorucci, L.; Polticelli, F.; Ascenzi, P.; Coletta, M.; Smulevich, G.; Santucci, R. The key role played by charge in the interaction of cytochrome c with cardiolipin. *J. Biol. Inorg. Chem.* **2017**, *22* (1), 19−29.
(64) Dai, D.-F.; Chiao, Y. A.; Marcinek, D. J.; Szeto, H. H.; Rabinovitch, P. S. Mitochondrial oxidative stress in aging and healthspan. *Longev. Heal.* **2014**, *3* (1), 6.
(65) Barros, M. H.; Netto, L. E. S.; Kowaltowski, A. J. H_2O_2 generation in Saccharomyces cerevisiae respiratory pet mutants: Effect of cytochrome c. *Free Radical Bio. Med.* **2003**, *35* (2), 179−188.
(66) Degli Esposti, M. Measuring mitochondrial reactive oxygen species. *Methods* **2002**, *26* (4), 335−340.
(67) Bodega, G.; Alique, M.; Puebla, L.; Carracedo, J.; Ramirez, R. M. Microvesicles: ROS scavengers and ROS producers. *J. Extracell. Vesicles* **2019**, *8* (1), 1626654.
(68) Murphy, M. P. How mitochondria produce reactive oxygen species. *Biochem. J.* **2009**, *417*, 1−13.
(69) Zhao, Y. G.; Wang, Z. B.; Xu, J. X. Effect of cytochrome c on the generation and elimination of O_2^- and H_2O_2 in mitochondria. *J. Biol. Chem.* **2003**, *278* (4), 2356−2360.
(70) Sinibaldi, F.; Howes, B. D.; Droghetti, E.; Polticelli, F.; Piro, M. C.; Di Pierro, D.; Fiorucci, L.; Coletta, M.; Smulevich, G.; Santucci, R. Role of Lysines in Cytochrome c-Cardiolipin Interaction. *Biochemistry* **2013**, *52* (26), 4578−4588.
(71) Burfield, D. R.; Law, K. S. Determination of carbonyl groups in polymers by reaction with 2,4-Dinitrophenylhydrazine. *Polymer* **1979**, *20* (5), 620−626.
(72) Wang, Z.; Ando, Y.; Nugraheni, A. D.; Ren, C.; Nagao, S.; Hirota, S. Self-oxidation of cytochrome c at methionine80 with molecular oxygen induced by cleavage of the Met-heme iron bond. *Mol. BioSyst.* **2014**, *10* (12), 3130−3137.
(73) Madeo, F.; Herker, E.; Wissing, S.; Jungwirth, H.; Eisenberg, T.; Frohlich, K. U. Apoptosis in yeast. *Curr. Opin. Microbiol.* **2004**, *7* (6), 655−660.
(74) Zhivotovsky, B.; Orrenius, S.; Brustugun, O. T.; Doskeland, S. O. Injected cytochrome c induces apoptosis. *Nature* **1998**, *391* (6666), 449−450.
(75) Shalaeva, D. N.; Dibrova, D. V.; Galperin, M. Y.; Mulkidjanian, A. Y. Modeling of interaction between cytochrome c and the WD domains of Apaf-1: bifurcated salt bridges underlying apoptosome assembly. *Biol. Direct* **2015**, *10*, 29.
(76) Zhou, M. Y.; Li, Y. N.; Hu, Q.; Bai, X. C.; Huang, W. Y.; Yan, C. Y.; Scheres, S. H. W.; Shi, Y. G. Atomic structure of the apoptosome: mechanism of cytochrome c- and dATP-mediated activation of Apaf-1. *Genes Dev.* **2015**, *29* (22), 2349−2361.

https://doi.org/10.1021/jacs.3c10216
J. Am. Chem. Soc. 2024, 146, 4455−4466